VOL. 16, NO. 23, DECEMBER 2021 ISSN 1819-6608
ARPN Journal of Engineering and Applied Sciences

www.arpnjournals.com

ASSESSMENT AND MODELING OF ELECTRIC FORCE IN A JIG DEVICE

Manuel A. Ospina-Alarcón[1], Liliana M. Úsuga-Manco[2], Gabriel E. Chanchí-Golondrino[1] and Santiago Gómez-Arango[3]
[1]Ingeniería de Sistemas, Facultad de Ingeniería, Universidad de Cartagena, Cartagena, Colombia
[2]Departamento de Educación y Ciencias Básicas, Facultas de Ciencias Exactas y Aplicadas, Instituto Tecnológico Metropolitano, Medellín, Colombia
[3]Departamento de Mecatrónica y Electromecánica, Facultad de Ingenierías, Instituto Tecnológico Metropolitano, Medellín, Colombia
E-Mail: mospinaa@unicartagena.edu.co

ABSTRACT

This paper presents a study of particle motion in a water oscillating flow on a Jig device, which is a high yield and high recovery gravimetric concentrator device widely used in minerals processing. The phenomenon of the particle trajectory changes when the electric field force exists. A mathematical Eulerian-Lagrangian model is used where fluid motion is calculated by solving the Navier-Stokes and continuity equations by a SIMPLE algorithm. The motion of individual particle is obtained from Newton's second law of motion through the action of forces imposed by the water, gravity, and electric field. The calculation and comparison of hydrodynamics forces with other forces acting on particle trajectories in water oscillating flows were carried out under turbulent regimen flow. Through the graphic observation in the simulation, it is found that the study found that electric field force has a significant effect on the particle's trajectories, affecting their subsequent stratification.

Keywords: solid-liquid interaction, gravimetric concentration, numerical simulation, high density suspensions, electric field.

INTRODUCTION

Jig is a gravity concentrator device in which mineral particles move relatively in a pulsating water flow resulting in a stratification of particles of different densities and sizes. In Figure-1 a schematic view of a Jig is given. Particle concentration inside de Jig happens in a complicated multiphase flow system. Particles are exposed to different forces in the fluid and results in different trajectories depending on the water velocity field and particles properties. Different operating variables will affect the trajectories of particles. They include feed water rate, amplitude (stroke length), and frequency (number of strokes per second) of oscillating flow (the stroke function. The fluid can be moved under a sinusoidal, a saw tooth or an asymmetrical function), the mineralogical content of a particle directly influences its density, surface characteristics, magnetic and electrical properties, among others [1]-[3]. These physical attributes in turn influence the behavior in the equipment that is designed to exploit differences in physical properties among the particles to effect a separation [4].

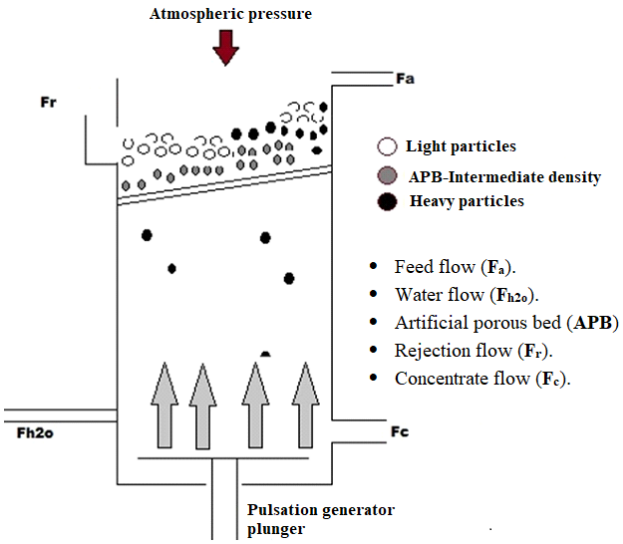

Figure-1. Jig schematic view [5].

Various models have been used to try to understand the gravimetric concentration process in Jigs. These models can be classified as following in two groups: potential energy theory [6]-[8] and DEM (discrete element method) approach [9]-[14].

Mayer [6] proposed his potential energy model. Based on this model, the potential energy difference between un-stratified and stratified particle bed is the drive force to cause separation. Tavares and King [8], made a modification of Mayer's theory to simulate the concentration of binary-sized feeds to overcome the limitation of Mayer´s model that can deal with uniform sized feed. However, it is still difficult for researchers to extend this model to the concentration of minerals

particles widely distributed in size and density. To obtain a quantitative analysis of concentration process in Jig, Mishra and Mehrotra [10], and Beck and Holtham [9] use a microscopic model in which the 2-D DEM is adopted. Srinivasan *et al*. [12] investigated a 3-D DEM model to simulate the stratification of particles in Jig bed. Mishra and Mehrotra [11] improved a 3-D DEM model by incorporating the new correlation of drag force to take account of bed porosity and validate their model against experimental data. In DEM models, the degree of stratification of bed can be quantified by determination of difference in the center of gravity between the particles of different densities [12] or by determination of decreasing speed of potential energy of Jig bed [9].

Above models treat the phenomenon assuming a uniform fluid field and did not consider the effect of possible non-uniform fluid velocity on particle hydrodynamic forces. Also, assume the stratification as a batch process and so far, there is no evidence of such investigations applying electric field to study particle stratification and subsequent equipment optimization. The addition of an electric force could become significant when calculating the trajectories followed by the particles entering the Jig separation chamber.

In general, existing theories provides a qualitative explanation of concentration process and contribute little to the designing of concentration equipment because an idealized fluid behavior is assumed. In this study, the mathematical Eulerian-Lagrangian model is used to simulate the particle trajectories fed to Jig. The motion of individual particle is traced as time progresses and, in this way, separation performance, size distribution, equipment recovery and enrichment ratio can be quantitatively determined.

The rest of the paper is organized as follows: section two presents the methodology considered for the development of this study through the Eulerian-Lagrangian model; section three presents the description of forces analysis through discussion of the results obtained; finally, section four presents the conclusions and future work derived from this research.

PROPOSED MODEL

The Euler-Lagrange model is used to calculate the water flow in a Euler frame where the particles are moved individually in Lagrangian coordinates. There are three stages in this approach incorporating the calculations of the water flow, solid particle movement and hydrodynamic interactions between water and solid particles. In the first part, the flow field is calculated from the balance equations of quasi-homogeneous solid-liquid dispersion where the mean density varies with the local particle concentration distribution. The water flow is obtained by solving the Navier-Stokes's equations using a suitable turbulent model [15]. In the second part, the motion of each particle is calculated in a Lagrangian frame of reference using the forces generated by water motion, gravity, and electric field. The local solid concentration is determined by tracking all individual particles of the system in the actual flow field and both steps are repeated until convergence is obtained. The effect of particles on the local flow field is then modeled at the third part, and this result is feedback into the flow field calculations at each time step [16]-[19].

Liquid Phase Hydrodynamics

The water velocity field is calculated by solving the dynamic conservation equations. Since no mass exchanges or chemical reactions are considered between water and minerals particles in the proposed model, the continuity equation of water can be formulated without the exchange term as follows in Eq. (1) [5], [10], [25], [11], [13], [14], [20]-[24]:

$$\frac{\partial}{\partial t}(\rho_l \phi_l) + \frac{\partial}{\partial x_i}(\rho_l \phi_l u_i) = 0 \tag{1}$$

The momentum balance for the water in multiphase flow is described in following general formulation by Eq. (2):

$$\frac{\partial}{\partial t}(\rho_l \phi_l u_i) + \frac{\partial}{\partial x_i}\left(\rho_l \phi_l u_i u_j\right) = -\frac{\partial P}{\partial x_i} + \frac{\partial}{\partial x_j}\Gamma\left(\frac{\partial u_i}{\partial x_j} + \frac{\partial u_j}{\partial x_i}\right) + \rho_l \phi_l g_i + F_{w_i} \tag{2}$$

$$\Gamma = \mu + \mu_t \tag{3}$$

In Eq. (1) and (2), ϕ_l, ρ_l and u are respectively, the water volume fraction in a computation cell, water density and water velocity component, P is the pressure, F_{wi} is momentum transfer term, g is the gravity acceleration and Γ in Eq. (3) is the viscosity composed of water viscosity μ and turbulent viscosity μ_t. The subscripts i and j represents coordinate axes directions. The k-ε model can be incorporated into the program to calculated water turbulent viscosity.

Particle Motion Equation

For mineral particles widely distributed in size and density, the description of the particle trajectories and interaction between the particles and water depends on the correct calculation of the hydrodynamic forces and the electric force involved. It is assumed that the forces acting on a solid spherical particle moving in a dynamic and non-uniform water flow field with the electric field are composed of separate and uncoupled contributions from the water drag force [26], the gravitational body force [27] and the electric force [28]-[31]. The Lagrangian equation of particle motion can be written in this approximation as Eq. (4) [13], [32], [33]:

$$m_p \frac{du_p}{dt} = -\frac{\pi}{8} C_d \rho_l d_p^2 \left|u_p - u_l\right|\left(u_p - u_l\right) + \cdots \ldots + \left(\rho_p - \rho_l\right) V_p g + QE \tag{4}$$

The three terms on the right-hand side of Eq. (4) are, in order from left to right, drag force, buoyancy force, and electric force, respectively. Where m_p, V_p, d_p, $\rho_p$are

the mass, the volume, the diameter, and the density of the particle, respectively, $\boldsymbol{u_p}$, $\boldsymbol{u_l}$ are particle and water velocities respectively, Q and E, are particle electric charge and electric field respectively, and C_d is the drag coefficient which for a spherical particle is a function of particle Reynolds numbers, expressed by Schiller and Naumann [34] correlation in the flow regime considered. In Eq. (4) three relevant parameters governing the motion of the particles are defined: the density ratio ($\chi=\rho_l/\rho_p$), the drag coefficient (C_d) and the electric field strength (E).

The calculation of particle trajectories requires the solution of tow ordinary differential equations, one for the calculation of the velocity (Eq. (5)) and one for the calculation of position (Eq. (6)) that in their vector form are:

$$m_{p_i} \frac{d\mathbf{u}_p}{dt} = \sum f_i \quad (5)$$

$$\frac{d\mathbf{x}_p}{dt} = u_p \quad (6)$$

where $\boldsymbol{f_i}$ represents the different relevant forces acting on a particle due to the interaction with the water and electric field. The trajectories of particles can be obtained by numerical integration of Eq. (5) and Eq. (6). The instantaneous water velocity components at the particle location required for calculation of forces in Eq. (4) are determined from the local mean water velocity interpolated from the neighboring Euler grid points using area weighted averaging techniques.

The lack of knowledge regarding the physical phenomenon of solid-fluid interaction, the need to develop adequate phenomenological models, the demand for high quality full-scale data, the need to develop data analysis techniques to better understand the results and the high cost of effective measurement devices by the industry are aspects that require numerical tools such as the one used in this investigation.

Solving of Navier-Stokes Equations by Simple Algorithm

Navier-Stokes Eq. (1) and Eq. (2) are solved by the ‘‘SIMPLE’’ (Semi-Implicit Method for Pressure Linked Equations) method in a 2D domain [35]. In this method, the partial differential equations for the mass and the momentum are solved by integrating the differential equations Eq. (1) and Eq. (2) over control volumes. For this, an orthogonal grid is applied (60x100 grids) where two velocities and pressures are stored in the staggered positions.

The linearization of the non-linear equations is performed by a ‘‘hybrid’’ difference method to get an implicit finite difference scheme. In this scheme, at a high Peclet number (Pe), it switches from central to upwind differencing for convection terms; for diffusion terms, the central differencing is used constantly. Due to of the elliptic nature of the partial differential equations, an iterative solution procedure is employed. Starting with guessed distributions for the velocity and pressure fields, the fluid velocities can be calculated from the momentum equation Eq. (2). Further, the pressure correction equation which has been derived from the continuity equation Eq. (1) is used to yield the corrected values for the velocity and the pressure fields so that the continuity equation is implicitly satisfied. With the corrected values, the momentum equations are solved again and the whole procedure is repeated until convergence is achieved [36], [37].

Solving of Particle Motion Equation by Runge-Kutta Method

Calculation of the particle trajectories by solving the equation of motion of the particles Eq. (4), as well as the calculation of the particle source terms, is performed in the same iteration loop after the solution of the water flow equations, in order to handle the iteration between the fluid and the particles. The change in particle velocity is calculated by integrating Eq. (5) and Eq. (6) via a fourth-order Runge-Kutta method at each time instant updating the position of particles after the interaction with the water [38].

Boundary Condition

The particle movement and water velocity field are simulated in a 2-D column with height of 0.1 m and width 0.05 m. The following assumptions were made regarding boundary conditions in this simulation:

- At the chamber Jig walls, water has non-slip conditions.
- The water inlet velocity at bottom of the column can be specified.
- The inlet water flow enters chamber from center of the bottom. The axial liquid velocity gradient at the bottom and at the top is zero.

RESULT ANS DISCUSSIÓNS

Particle trajectory patterns that can help to understand the stratification process inside the Jig separation chamber are reviewed. The model was simulated in two software applications, MATLAB®(R2019b) and ANSYS Fluent R2(2020) using an user define function (UDF) to couple the water velocity field and the Runge Kutta method to calculate the particle trajectories, these programs were installed in a computer with an 4-core processor and 8GB of RAM. We used a sampling time t_s=0.01 s.

The influence of each force in the particle trajectory equation was developed for different particle sizes and densities in pulsating water flow. The particles were pulsated into a 5 x 10 cm^2 area injected from a position x=0.048 m and y=0.048 m. A sinusoidal type of waveform was imparted to the water, where the amplitude and frequency of oscillation velocity were set at 0.08816 m/s and 5 Hz, respectively. The motion equation of particles is obtained from Newton’s second law of motion (Eq. (4)). The most basic form of the model contains the drag and buoyancy forces that significantly driving the particle motion. Tables 1 to 3 show the calculation of the

electric force for different particle sizes (d_p=125µm, d_p=300µm and d_p=850µm) and densities (from ρ_p =3029 kg/m3 to ρ_p =13000 kg/m3). These values are then added to the simulation model by the trajectory equation (Eq. (4)).

Table-1. Particle diameter 125 µm characterized with its electrical force.

Particle density (kg/m^3)	Q (C)	Electric force(N)
3188.7	-1.26E-01	-6.30E-06
3226.4	-1.27E-01	-6.37E-06
3308.7	-1.31E-01	-6.54E-06
3562.5	-1.41E-01	-7.04E-06
4089	-1.62E-01	-8.08E-06
4299.8	-1.70E-01	-8.50E-06
13000	-5.14E-01	-2.57E-05

Table-2. Particle diameter 300 µm characterized with its electrical force.

Particle density (kg/m^3)	Q (C)	Electric force (N)
3188.7	-1.74	-8.71E-05
3226.4	-1.76	-8.81E-05
3308.7	-1.81	-9.04E-05
3562.5	-1.95	-9.73E-05
4089	-2.23	-1.12E-04
4299.8	-2.35	-1.17E-04
13000	-7.10	-3.55E-04

Table-3. Particle diameter 850 µm characterized with its electrical force.

Particle density (kg/m^3)	Q (C)	Electric force (N)
3188.7	-3.96E+01	-1.98E-03
3226.4	-4.01E+01	-2.00E-03
3308.7	-4.11E+01	-2.06E-03
3562.5	-4.43E+01	-2.21E-03
4089	-5.08E+01	-2.54E-03
4299.8	-5.34E+01	-2.67E-03
13000	-1.62E+02	-8.08E-03

The results of these analyses are shown in Figures 2 to 4. In Figure-1 the particles have a uniform size of 125 µm with a density of 3029 kg/m^3. The fluidization velocity of the water is 5.841 cm/s and solid concentration is about 6% at a time instant t=5 s. Figure-2a shows the effect of the drag and buoyancy forces on the particle trajectory, while Figure-2b has the addition of the electric force. It was shown that the drag force and buoyancy force are not dominant forces because when the electric force is added, the particle completely changes its trajectory switching from the rejection current to the concentrate current. Also, in Figures 2 to 4 it can be seen that as the density increases, the electric force significantly influences not only the movement of the particles but also affects the residence time of the mineral and its subsequent concentration, indicating that the concentration process could be significantly improved in terms of energy consumption of the devices involved in the process such as motors and vibrating screens.

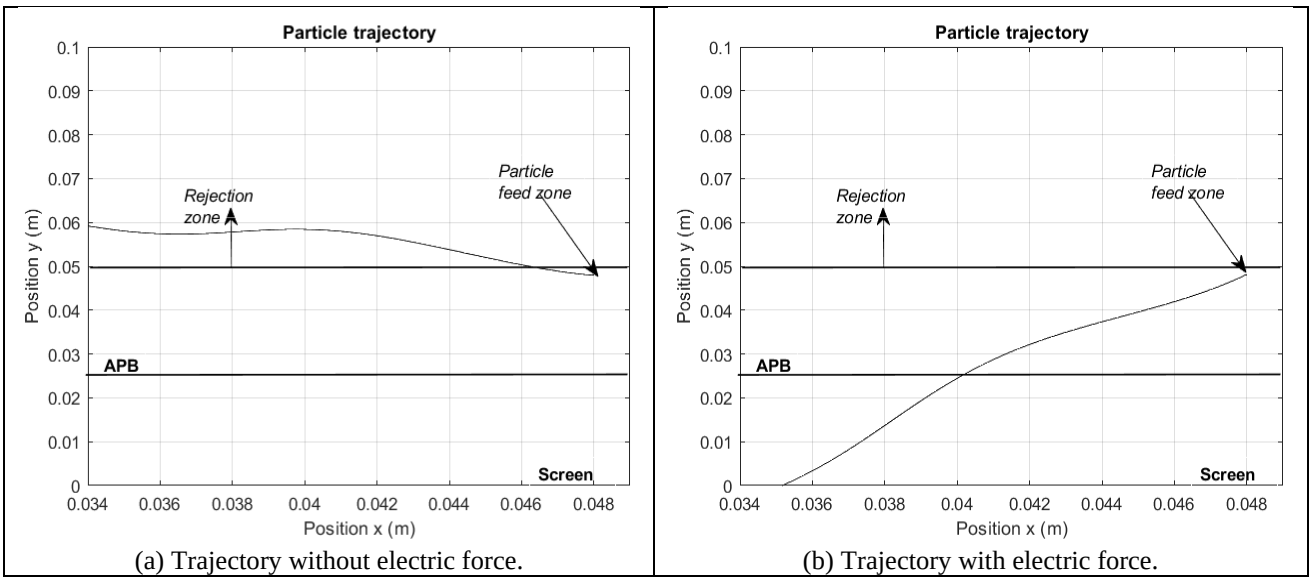

(a) Trajectory without electric force. (b) Trajectory with electric force.

Figure-2. Particle Trajectory, diameter 125 µm and density 3029 kg/m^3.

From Figure-2 particles with the specified size and density will be reported in the reject stream if only the drag and buoyancy forces are considered, but with the addition of the electric force the fine particles of the mineral could be directed towards the concentrate stream avoiding mineral losses and significantly improving the metallurgical indexes of the concentrator equipment. The same pattern can be seen in Figures 3 and 4, for particle size and density configurations of 300 μm and 3402 kg/m^3, and 850 μm and 13000 kg/m^3, respectively. The forces acting on the particle trajectory in gravimetric concentration device vary with particle size, particle density and suspension properties. Electric force significantly affects particle trajectories inside the Jig chamber.

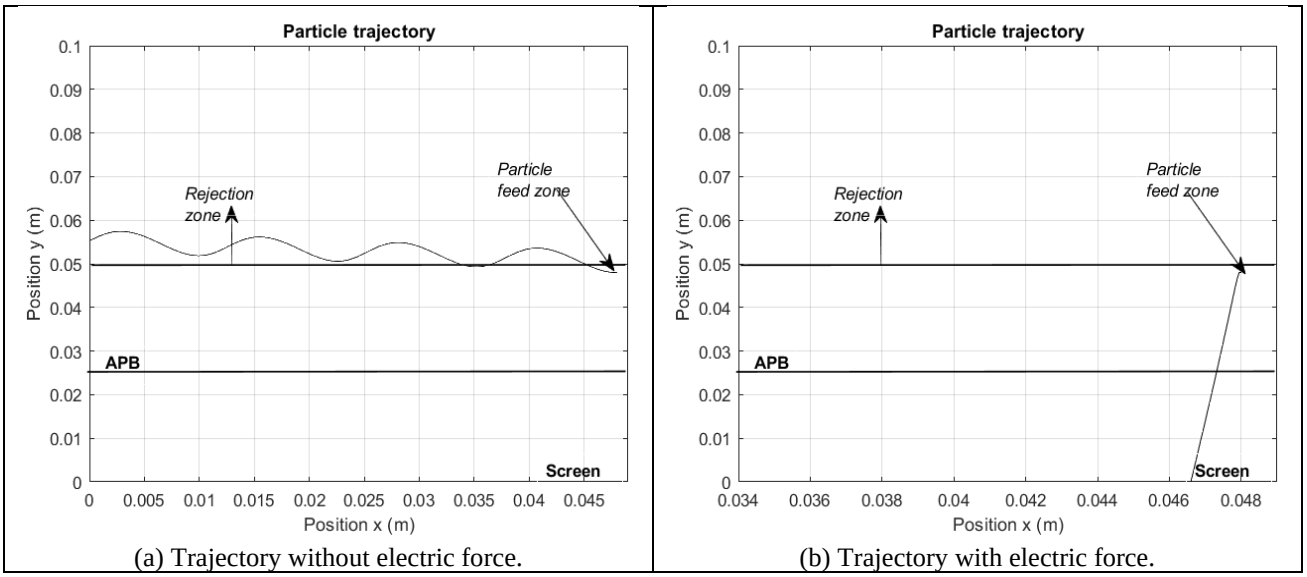

(a) Trajectory without electric force. (b) Trajectory with electric force.

Figure-3. Particle Trajectory, diameter 300 μm and density 3402 kg/m^3.

Figures 2 to 4 show the trajectory followed by the particles inside the Jig column. Particles with a diameter greater than 300 μm and a density greater than 3562 kg/m^3 stratify completely without the action of the electric force (Figure-4a), but fine particles (smaller than 300 μm) will stratify if they are directly influenced by the electric force (Figures 2b and 3b). A more general analysis of Figures 2 to 4 shows that the residence time of particles in the Jig chamber is quite sensitive to the applied electric force, particle size and particle density. A particle of density ρ<3563 kg/m^3 will exit faster and through the concentrate stream when an electric force is applied (Figures 2b, 3b and 4b) than when no electric force is applied (Figures 2a, 3a and 4a). On the contrary, if the density is ρ>3563 kg/m^3, the particle will remain for a shorter time when an electric force is applied (Figures 2b and 4b), significantly affecting its trajectory, directing it towards the concentrate stream.

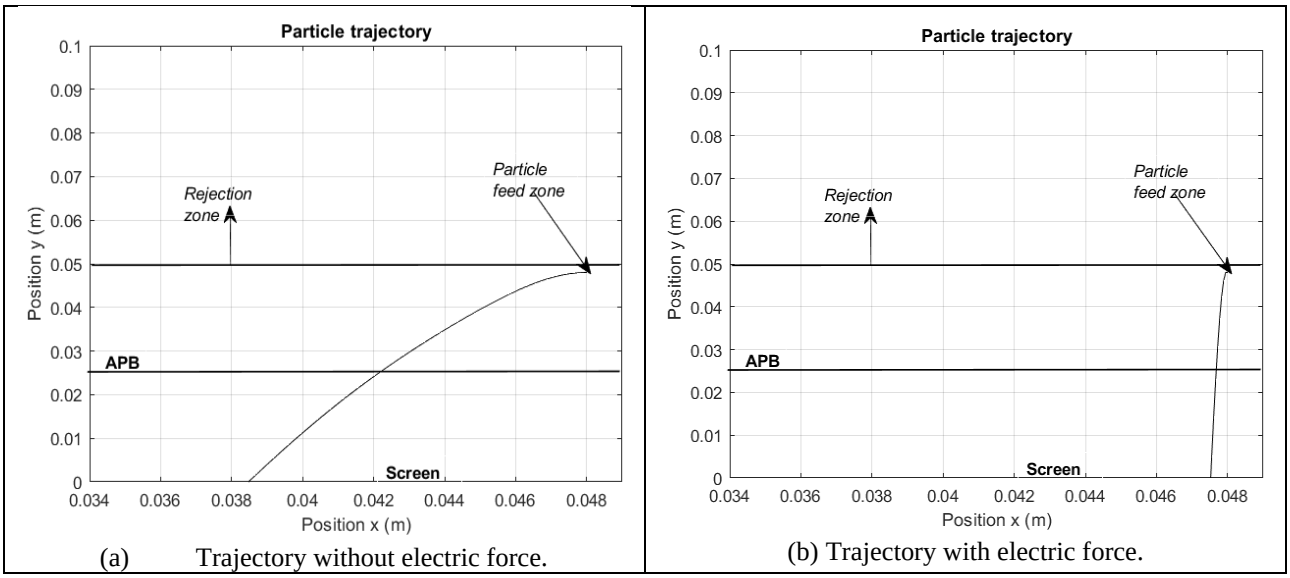

(a) Trajectory without electric force. (b) Trajectory with electric force.

Figure-4. Particle Trajectory, diameter 850 μm and density 13000 kg/m^3.

Finally, it could be demonstrated from Figures 2 to 4, that neglect the electric force on particle motion model for pulsating beds do not generate a good explanation of the phenomenon of solid-liquid interaction in gravimetric concentrations device.

The position in the vertical direction of each type of particle provides a good understanding of the gravimetric concentration process in Jigs. Starting from an initial condition where each type of particle is injected from the same position and at the same velocity, the light particles move upwards much faster than the heavy particles during the fluidization period. During the suction period, all particles fall, but the heavier particles fall much faster than the lighter particles. The above results suggest that to improve the performance of the concentrator equipment, in terms of recovery, enrichment ratio and time and energy consumption, an experimental analysis and evaluation of a Jig with the addition of an electric field is necessary to validate the results of this study.

CONCLUSIONS

The trajectory of mineral particles in a Jig under the effect of an electric field was studied using the Eulerian-Lagrangian mathematical model with the amplitude and frequency of pulsation at a constant value. The addition of electric force can stratify mineral particles that have a fine size (less than 125 μm) and intermediate densities, also subject to shorter separation times (shorter residence time).

The particle trajectory is a function of particle size, particle density and suspension properties by calculations of isolated heavy particles. Although it was found that the drag force, buoyancy force are not dominant forces in determination of particle motion. It was determined in this study that the effect of electric force on particles trajectories inside the artificial porous Jig bed (APB) in a non-uniform pulsating flow are significant, representing particle stratification inside the Jig bed (APB) a more accurate way. It was determined that the particle trajectory (defining the size and density separation) is a consequence of the fluid flow field.

The mathematical model described in this paper has given more insight in the behavior of particles trajectories in a Jig, in terms of the forces like buoyant, drag and electric, but the description of the entire jigging process with respect to stratification of particles to be separated was not possible. To use the model for the description of the segregation process in the Jig it has to be extended to a multi component system and the equations of interaction among particles have to be added to the mathematical equation of model.

The particle trajectory is calculated once the fluid velocity contours are simulated. It should be clarified that for both research and industrial purposes, more simulations involving different types of pulsation should be carried out and the respective validation with experimental data, either in a laboratory, pilot plant or industrial scale tests that allow us to affirm that the simulation results are suitable to be applied to gravity separation problems in the mining industry.

From the results, a study involving the interaction between the particles (particle-particle interaction forces or so-called solid-solid contact forces) is necessary for a more detailed understanding of the operation of the concentrator equipment. However, the research demonstrates the usefulness of the Eulerian-Lagrangian model as an effective numerical model to study the gravity concentration process in Jigs. Additional research is required that considers different amplitudes and pulsation periods, in addition to testing in simulation other pulsation profiles different from the sinusoidal, as well as a validation with experimental tests that will help to understand and optimize the performance of the equipment by means of the physical conservation principles that govern it. Future research implementing advanced control functions by using machine vision and multivariate data analysis are necessary. Further investigation is needed in order to evaluate the practical feasibility of such methods.

ACKNOWLEDGMENTS

Authors are grateful for the support of simulations works by project "Diseño y modelamiento de un concentrador gravimétrico con campo eléctrico para la recuperación de minerals" with ID P20221. Materiales Avanzados y Energía (MATYER) and Automática y Electrónica groups at the Instituto Tecnológico Metropolitano, Medellín-Colombia, and the Systems Engineering program of the Universidad de Cartagena, for their support in the financing, use of equipment and advice provided by the researchers.

REFERENCES

[1] W. M. Ambrós. 2020. Jigging: A review of fundamentals and future directions. Minerals, 10(11): 1-29, doi: 10.3390/min10110998.

[2] W. M. Ambrós, C. H. Sampaio, B. G. Cazacliu, G. L. Miltzarek and L. R. Miranda. 2017. Usage of air jigging for multi-component separation of construction and demolition waste. Waste Manag., 60: 75-83, doi: 10.1016/j.wasman.2016.11.029.

[3] R. O. Burt and C. Mills. 1984. Gravity concentration technology, Vol. 5. Amsterdam, Netherlands: Elsevier.

[4] R. P. King. 2001. Introduction. in Modeling and Simulation of Mineral Processing Systems. pp. 1-4.

[5] M. A. Ospina and M. O. Bustamante. 2015. Hydrodynamic study of gravity concentration devices type JIG. Rev. Prospect., 13(1): 52-58, doi: http://dx.doi.org/10.15665/rp.v13i1.359.

[6] F. W. Mayer. 1964. Fundamentals of a potential theory of jigging process. in 7th International Mineral Processing Congress. pp. 75-86.

[7] G. J. Lyman. 1992. Review of Jigging Principles and Control. Coal Prep., 11(3-4): 145-165, doi: 10.1080/07349349208905213.

[8] L. M. Tavares and R. P. King. 1995. A Useful Model for the Calculation of the Performance of Batch and Continuous Jigs. Coal Prep., 15(3-4): 99-128, doi: 10.1080/07349349508905291.

[9] A. J. Beck and P. N. Holtham. 1993. Computer simulation of particle stratification in a two-dimensional batch jig. Miner. Eng. 6(5): 523-532.

[10] B. K. Mishra and S. P. Mehrotra. 1998. Modelling of particle stratification in jigs by the discrete element method. Miner. Eng. 11(6): 511-522.

[11] B. K. Mishra and S. P. Mehrotra. 2001. A jig model based on the discrete element method and its experimental validation. Int. J. Miner. Process, 63: 177-189, doi: 10.1016/S0301-7516(01)00053-9.

[12] R. Srinivasan, B. K. Mishra and S. P. Mehrotra. 1999. Simulation of Particle Stratification in Jigs Simulation of Particle Stratification in Jigs. Coal Prep., 20(1-2): 55-70, doi: 10.1080/07349349908945592.

[13] S. Viduka, Y. Feng, K. Hapgood and P. Schwarz. 2013. CFD-DEM investigation of particle separations using a sinusoidal jigging profile. Adv. Powder Technol., 24(2): 473-481, doi: 10.1016/j.apt.2012.11.012.

[14] Y. Xia, F. F. Peng and E. Wolfe. 2007. CFD simulation of fine coal segregation and stratification in jigs. Int. J. Miner. Process, 82(3): 164-176, doi: 10.1016/j.minpro.2006.10.004.

[15] B. Mohammadi and O. Pironneau. 1994. Analysis of the k-epsilon turbulence model. New York: Jonh Wiley & Sons.

[16] H. P. Zhu, Z. Y. Zhou, R. Y. Yang and A. B. Yu. 2008. Discrete particle simulation of particulate systems: A review of major applications and findings. Chem. Eng. Sci., 63(23): 5728-5770, doi: 10.1016/j.ces.2008.08.006.

[17] K. Asakura, S. Harada, T. Funayama and I. Nakajima. 1997. Simulation of descending particles in water by the distinct element method. Powder Technol. 94: 195-200.

[18] K. Asakura, M. Mizuno, M. Nagao and S. Harada. 2007. Numerical Simulation of Particle Motion in a Jig Separator. in 5th Join ASME JSME Fluids Engineering Conference. pp. 385-391.

[19] K. Asakura, M. Nagao and M. Mizuno. 2007. Simulation of Particle Motion in a Jig Separator. J. JSEM. 7(Special Issue).

[20] L. M. Chica, M. A. Ospina and M. Bustamante. 2012. Uso de CFD para la simulación de procesos mineralúrgicos de concentración gravimétrica. 10(1): 85-96.

[21] S. Cierpisz. 2017. A dynamic model of coal products discharge in a jig. Miner. Eng., 105: 1-6, doi: 10.1016/j.mineng.2016.12.010.

[22] D. Markauskas, H. Kruggel-Emden and V. Scherer. 2018. Numerical analysis of wet plastic particle separation using a coupled DEM-SPH method. Powder Technol., 325: 218-227, doi: 10.1016/j.powtec.2017.11.021.

[23] M. A. Ospina. 2014. Modelamiento de la hidrodinámica de la separación gravimétrica de minerales en jigs. Universidad Nacional de Colombia.

[24] M. A. Ospina, A. B. Barrientos and M. O. Bustamante. 2016. Influence of the pulse wave in the stratification of high-density particles in a JIG device. Rev. Tecno Lógicas. 19(36): 13-25.

[25] M. A. Ospina and L. M. Usuga. 2018. Effect of Hydrodynamic forces on mineral particles trajectories in Gravimetric concentrator Type Jig. Politecnica. 14(27): 68-79.

[26] A. B. Basset. 1988. A Treatise on Hidrodynamics, Volumen II. London, UK: George Bell and Sons.

[27] Y. K. Xia and F. F. Peng. 2007. Numerical simulation of behavior of fine coal in oscillating flows. Miner. Eng., 20(2): 113-123, doi: 10.1016/j.mineng.2006.06.004.

[28] G. Saccone, A. I. Garivalis and P. Di Marco. 2020. Electrohydrodynamics and boiling: Experiments, numerical calculation and modeling of Maxwell stress tensor and electric force acting on bubbles. J. Electrostat., 103(August 2017): 103413, doi: 10.1016/j.elstat.2019.103413.

[29] H. W. Li, Y. C. Wang, C. H. Du and W. P. Hong. 2021. Analysis of flow pattern change in horizontal mini-channel under electric field force. Int. Commun. Heat Mass Transf., 121(December 2020): 105081, doi: 10.1016/j.icheatmasstransfer.2020.105081.

[30] D. S. Correnti. 2018. Mechanisms explaining Coulomb's electric force & Lorentz's magnetic force from a classical perspective. Results Phys., 9: 832-841, doi: 10.1016/j.rinp.2018.03.027.

[31] R. J. Singh and T. B. Gohil. 2019. The numerical analysis on the variation of electric potential, electric current and Lorentz force with its influence on buoyancy-driven conjugate heat transfer and fluid flow using OpenFOAM. Fusion Eng. Des., 148(September): 111300, doi: 10.1016/j.fusengdes.2019.111300.

[32] S. M. Viduka, Y. Q. Feng, K. Hapgood and M. P. Schwarz. 2013. Discrete particle simulation of solid separation in a jigging device. Int. J. Miner. Process, 123: 108-119, doi: 10.1016/j.minpro.2013.05.001.

[33] S. M. Viduka, Y. Q. Feng, K. Hapgood and M. P. Schwarz. 2012. CFD-DEM investigation of particle separations using a Trapezoidal jigging profile. in Ninth International Conference on CFD in the Minerals and Process Industries, pp. 1-8, doi: 10.1016/j.apt.2012.11.012.

[34] L. Schiller and A. Naumann. 1933. Über die grundlegenden Berechnungen bei der Schwerkraftaufbereitung. Ver. Deut. Ing., 77: 318-320.

[35] H. K. Versteeg and W. Malalasekera. 2007. An Introduction to Computational Fluid Dynamics, 2nd ed. London, UK: Pearson Education.

[36] S. V. Patankar and D. B. Spalding. 1972. A calculation procedure for heat, mass and momentum transfer in three-dimensional parabolic flows. Int. J. Heat Mass Transf., 15(10): 1787-1806, doi: 10.1016/0017-9310(72)90054-3.

[37] S. V. Patankar. 1980. Numerical Heat Transfer and Fluid Flow. New York: Hemisphere Publishing Corporation.

[38] M. Sommerfeld and N. Huber. 1999. Experimental analysis of modelling of particle-wall collisions. Int. J. Multiph. Flow, 25(6-7): 1457-1489, doi: 10.1016/S0301-9322(99)00047-6.